Solid State Ionics xxx (2015) xxx–xxx

Contents lists available at ScienceDirect

Solid State Ionics

journal homepage: www.elsevier.com/locate/ssi

XRD and XAFS study on structure and cation valence state of layered ruthenium oxide electrodes, Li_2RuO_3 and $Li_2Mn_{0.4}Ru_{0.6}O_3$, upon electrochemical cycling

Daisuke Mori [a,*], Hironori Kobayashi [b], Toyoki Okumura [b], Hiroaki Nitani [c], Masahiro Ogawa [d], Yoshiyuki Inaguma [a]

[a] Department of Chemistry, Faculty of Science, Gakushuin University, 1-5-1 Mejiro, Toshima-ku, Tokyo 171-8588, Japan
[b] Research Institute for Electrochemical Energy, National Institute of Advanced Industrial Science and Technology (AIST), 1-8-31 Midorigaoka, Ikeda, Osaka 563-8577, Japan
[c] Institute of Materials Structure Science, High Energy Accelerator Research Organization (KEK), 1-1 Oho, Tsukuba, Ibaraki 305-0801, Japan
[d] Research Organization of Science and Engineering, Ritsumeikan University, 1-1-1 Nojihigashi, Kusatsu, Shiga 525-8577, Japan

ARTICLE INFO

Article history:
Received 18 April 2015
Received in revised form 17 August 2015
Accepted 25 September 2015
Available online xxxx

Keywords:
Lithium battery
Li_2MnO_3
Li_2RuO_3
Li-rich manganese layered oxide
XANES
Local structure

ABSTRACT

Structure and valence state change of Li_2RuO_3 and ruthenium-substituted lithium manganese oxide, $Li_2Mn_{0.4}Ru_{0.6}O_3$ (LMR), with layered structure were investigated using Synchrotron X-ray diffraction (SXRD) and X-ray absorption spectroscopy measurements before and after electrochemical cycling. The charge–discharge voltage curves of both LMR and Li_2RuO_3 significantly vary in the subsequent cycle. The SXRD Rietveld structural refinements demonstrate that the LMR undergoes irreversible structural transition. The Mn K-edge spectra confirm the structural modification in the MnO_6 octahedra with Li de-intercalation. The Ru L-edge spectra for LMR show similar behavior to Li_2RuO_3 during electrochemical cycling. These spectra appear reductive peak shift on the way to charging to 4.8 V. The phenomena are not attributed to the reduction of hexavalent Ru to pentavalent but a variation of the splitting between bonding and anti-bonding e_g orbitals. The charge–discharge reactions mechanism of LMR and Li_2RuO_3 are discussed.

1. Introduction

Much attention has been inclined to lithium batteries as indispensable energy storage technologies, not only for portable electronic devices but also for hybrid and pure electric vehicles. Li_2MnO_3 is a promising candidate as an alternative cathode material having higher voltage, larger theoretical capacity of about 460 mAh g^{-1} taking into account that all lithium ions are utilized, lower cost and lower environmental impact. Li_2MnO_3 synthesized by usual solid-state reaction practically shows poor electrochemical properties and high discharge capacity is achieved by reducing particle size and oxygen removal treatments [1–5]. The Li-rich manganese layered oxide Li_2MnO_3–$LiMO_2$ (M = 3d transition metal) systems have been widely examined and are the most promising candidates [6–8]. Among them, the Li_2MnO_3–$LiMn_{0.5}Ni_{0.5}O_2$ system delivered larger initial capacities than 250 mAh g^{-1} [6]. Li-rich manganese layered oxides exhibit a distinct voltage plateau in which a structural rearrangement undergoes due to oxygen evolution and cation migration [9–11]. However, the incompatible structural character between Li_2MnO_3 and $LiMO_2$ phases provides complex layered structure on the nano-metric level with complicated cation distribution [12,13]. The mechanism underlying the higher capacity is a major focus of interest for the past several years but the detailed mechanism has not been sufficiently clarified.

Previously, we successfully synthesized the solid solution of Li_2MnO_3–Li_2RuO_3 and investigated its phase relation, structure, electrical property and electrochemical property depending on the Ru content [14]. Li_2RuO_3 is isostructural with Li_2MnO_3, composed of lithium and lithium-transition metal layer except for a minor stacking difference. In addition, Li_2RuO_3 exhibits complementary properties to Li_2MnO_3 such as good cyclic capacity of about 160 mAh g^{-1} and remarkably lower resistivity of 10 Ω cm [15,16]. Our study found that substitution of Ru is effective to enhance the electrochemical as well as electrical properties [14]. The Mn K-edge spectra of $Li_2Mn_{1-x}Ru_xO_3$ showed a different behavior from other Li-rich manganese layered oxides upon electrochemical cycling in a preliminary study, which is conceivably correlated with the Ru reduction or oxygen oxidation [17]. Recently, Sathiya et al. conducted a systematic study on the charge compensation mechanism of $Li_2Ru_{1-x}M_xO_3$ (M = Mn, Sn) by using X-ray photoelectron spectroscopy (XPS) and electron paramagnetic resonance [18,19], and addressed that a reversible anionic redox process is the origin of the high capacity in these systems. Moreover, the anionic redox process in $Li_2Ru_{1-x}Sn_xO_3$ is involved in the reductive coupling in which the hexavalent Ru is reduced due to the clearage of Ru–O bond

* Corresponding author.
E-mail address: daisuke.mori@gakushuin.ac.jp (D. Mori).

http://dx.doi.org/10.1016/j.ssi.2015.09.025
0167-2738/

accompanied with the formation of a peroxo-like ion $(O_2)^{2-}$ [19]. However, the mechanistic study has not been sufficiently done for Li_2RuO_3 and its related materials. Even Li_2RuO_3 as an end member of the $Li_2Ru_{1-x}M_xO_3$ (M = Mn, Sn) has been limited to a few studies on electrochemical property [15,16,20–22] and using epitaxial film electrode [23–26]. In this study, we discuss the variation of average and local structure and valence state of cations upon the initial intercalation/de-intercalation of Li_2RuO_3 and $Li_2Mn_{0.4}Ru_{0.6}O_3$ ($x = 0.6$; hereafter denoted as LMR) showing the largest specific capacity and good cyclic property among $Li_2Mn_{1-x}Ru_xO_3$ system by using the ex-situ X-ray diffraction (XRD) and X-ray absorption near edge structure (XANES) measurements.

2. Experimental

The LMR and Li_2RuO_3 were synthesized by a solid-state reaction at 1200 °C and 1000 °C, respectively, as reported previously [14] and phase identification was done by the XRD measurement with Rigaku RINT 2100 diffractometer using monochromatic Cu Kα line. The electrochemical properties were examined using 2032-type-coin-cells (Hohsen Corp.) under a voltage range from 2.0 V to 4.8 V vs. Li/Li^+ at a constant current rate of C/10 calculated from the theoretical capacity taking only into account that Li in lithium layer is utilized. The positive electrode was composed of the active material, acetylene black (HS-100, DENKA) and poly(vinylidene difluoride) (PVdF) binder (KISHIDA CHEMICAL Co., Ltd.) with a weight ratio of 10:1.5:1.5 and coated onto Al current collector. 1 M $LiPF_6$ in ethylene carbonate/diethyl carbonate (EC/DEC) with a volume ratio of 3:7 (KISHIDA CHEMICAL Co., Ltd.) and Li metal foils were used as the electrolyte and the negative electrode, respectively. The cell was disassembled after the electrochemical test and the obtained electrode was washed by DEC and then dried in an Ar filled glove box.

Synchrotron XRD (SXRD) data were collected on a Debye–Scherrer-type powder diffractometer with an imaging-plate (IP) type detector installed in the beamline BL02B2 at SPring-8. The incident synchrotron radiation was calibrated with a CeO_2 standard. The X-ray of wavelength $\lambda = 0.6004(1)$ Å and 0.6005(1) Å was used for the data collection of LMR and Li_2RuO_3, respectively. The sample was packed into a glass capillary of 0.4 mm in the outer diameter after exfoliation from current collector. The structural parameters were refined by the Rietveld analysis using the program RIETAN-FP [27] and the crystal structure was drawn using the program VESTA [28]. The Mn K-edge XANES spectra were measured in the transmission mode in the beamline BL9C at Photon Factory (PF) in High Energy Accelerator Research Organization (KEK). The samples were sealed into polyethylene or polypropylene films. The Ru L-edge XANES spectra measurements were performed in the total electron yield (TEY) and fluorescence yield (FY) mode in BL-10 at SR center in Ritsumeikan University. The obtained samples were transported to the chamber using the sealed vessel filled with Ar.

3. Results

3.1. Charge–discharge behavior for LMR

The representative charge–discharge voltage curves from the initial to the second cycle for LMR and Li_2RuO_3 are shown in Fig. 1. A two-stage process consisting of a slope around 3.7 V and a plateau at 4.25 V was observed in the initial charge process of LMR. Approximately 0.6 Li was extracted at 4.2 V, indicating the oxidation of Ru^{4+} to Ru^{5+} (see Section 3.3). The plateau at 4.25 V would be associated with simultaneous Li^+ and O^{2-} removal [29], cation migration [10,11] and/or oxidation of oxygen [30]. The initial charge capacity was greater than theoretical one (278 mAh g^{-1}). The discharge curve did not show any plateau region as seen in the charge curve and the irreversible capacity was observed. Subsequently, the voltage increased monotonously in the second charge. The substantial variation of charge voltage curve

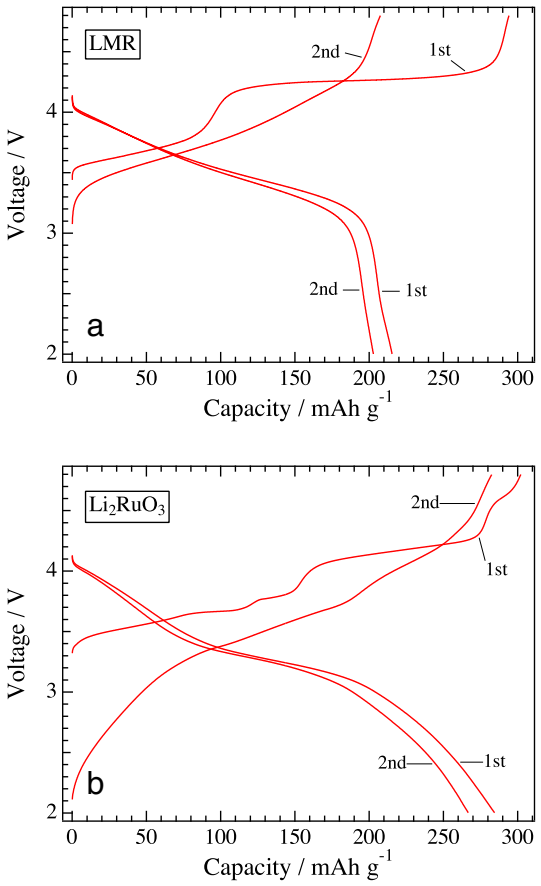

Fig. 1. Charge–discharge profiles of LMR (a) and Li_2RuO_3 (b).

between the initial and second charges was clearly observed. Moreover, similar profile of discharge curve to the initial cycle was observed in the second discharge process.

The initial charge and discharge capacities for Li_2RuO_3 delivered 300 and 285 mAh g^{-1}. The much higher discharge capacity corresponding to 1.7 Li and lower irreversible capacity than those of LMR were obtained in the initial cycle. Li_2RuO_3 exhibited attractive electrochemical property. The charge voltage curve has two plateaus in the initial cycle to 4.0 V [16]. The additional plateaus were observed around 4.15 V and 4.6 V. The discharge curve showed indistinct plateau-like regions around 3.3 V, which is not similar to that of LMR. The substantial variation of charge curves between the initial and second charge was also observed clearly. Moreover, similar profile of discharge curve to initial cycle was observed in the second discharge process. These features for LMR and Li_2RuO_3 suggest that the Li (de-) intercalation mechanism varies in the initial charge process accompanied with the variation of crystal structure and electronic state. Therefore, ex-situ XRD and XANES measurements were conducted for LMR in comparison with Li_2RuO_3.

3.2. Phase transition with electrochemical cycling

The SXRD patterns for LMR and Li_2RuO_3 before and after electrochemical cycling are shown in Fig. 2. The diffraction patterns correspond to the pristine, the initial charge and discharge and then second charge and discharge process in sequence from the bottom. The LMR showed the shift of reflections in complicated manner, peak broadening and reversible evolution of new peaks upon charge and discharge cycling. The diffraction pattern of pristine LMR sample was indexed with the space group $C2/m$ similar to Li_2MnO_3 [14]. With the initial charge to 4.0 V, the 220 reflection evolved at lower angle side of 131 reflection.

Please cite this article as: D. Mori, et al., XRD and XAFS study on structure and cation valence state of layered ruthenium oxide electrodes, Li_2RuO_3 and $Li_2Mn_{0.4}Ru_{0.6}O_3$, upon electrochemical cycling, Solid State Ionics (2015), http://dx.doi.org/10.1016/j.ssi.2015.09.025